Archaeological and Anthropological Sciences (2019) 11:1391–1405
https://doi.org/10.1007/s12520-017-0593-3

ORIGINAL PAPER

The anomaly of glass beads and glass beadmaking waste at Jiuxianglan, Taiwan

Kuan-Wen Wang[1,2] · Yoshiyuki Iizuka[3] · Yi-Kong Hsieh[4] · Kun-Hsiu Lee[5] · Kwang-Tzuu Chen[2] · Chu-Fang Wang[4] · Caroline Jackson[1]

Received: 1 November 2017 / Accepted: 26 December 2017 / Published online: 17 February 2018

Abstract

Glass beads and beadmaking waste have been excavated at the Iron Age site of Jiuxianglan (ca. third century BC–eighth century AD) in southeastern Taiwan. It was suggested that this site may be a production and exchange centre of glass beads in Iron Age Taiwan. This paper presents the analysis of 44 samples, to explore the relationship between glass beads and waste and the nature of bead production at Jiuxianglan. The analysis combines data on style, chemical composition, microstructure and distribution of glass beads and waste. The results do not show a compositional or structural match between the glass beads and glass waste, suggesting that the glass beads may not have been produced at this site.

Keywords Glass bead · Glass waste · Iron Age · Taiwan · Chemical composition · Microstructure

Introduction: the Jiuxianglan site and the glass finds

Jiuxianglan (舊香蘭) is located on the south bank of the estuary of the Taimali Stream in southeastern Taiwan (Fig. 1). C-14 dating has shown an occupation period between the third century BC and eighth century AD (Lee 2005b: 168; 2010: 30–31; 2015b: 182–183). The rescue excavations in the early 2000s show it was occupied by the Iron Age Sanhe Culture (三和文化) (see Liu et al. 1994 and Liu 2011: 248–251 for reference to the Sanhe Culture), which is characterised by the presence of iron artefacts, glass beads and pottery with triangular handles and punch-dotted motifs, which were found at the site (Lee 2010: 171–183). In addition, the vessel shapes and motifs of some funerary pottery found from Jiuxianglan are similar to those found in the Guishan Culture in southernmost Taiwan (Lee 2010: 182–183), which may indicate some interaction or cultural affinities to the cultures in southern Taiwan.

The presence of significant numbers of glass beads and Southeast Asian style sandstone moulds may suggest interaction with contemporary Southeast Asia. The physical appearance of the glass beads from Jiuxianglan resembles the monochrome glass beads from the Indo-Pacific (e.g. Francis 2002, colour plate 9; Hung and Bellwood 2010: 242; Lankton et al. 2003: 69). The excavations at Jiuxianglan also found bivalve sandstone moulds used for casting objects in bronze and possibly precious metals, and it has been suggested that the style of these casting moulds is similar to clay-made moulds found in Southeast Asia (Hung and Bellwood 2010; Hung and Chao 2016), although investigation of the sandstone used to produce the moulds indicates this raw material was procured locally in southern Taiwan (Yang et al. 2012).

One of the striking finds at Jiuxianglan was the first reported evidence for pyrotechnology relating to glass beadmaking

Electronic supplementary material The online version of this article (https://doi.org/10.1007/s12520-017-0593-3) contains supplementary material, which is available to authorized users.

✉ Kuan-Wen Wang
kwnwang@asihp.net

✉ Caroline Jackson
c.m.jackson@sheffield.ac.uk

[1] Department of Archaeology, University of Sheffield, Minalloy House, 10-16 Regent Street, Sheffield S1 3NJ, UK

[2] Institute of History and Philology, Academia Sinica, No. 130, Section 2, Academia Road, Nangang, Taipei 11529, Taiwan

[3] Institute of Earth Sciences, Academia Sinica, No. 128, Section 2, Academia Road, Nangang, Taipei 11529, Taiwan

[4] Department of Biomedical Engineering and Environmental Sciences, National Tsing Hua University, No. 101, Section 2, Kuang-Fu Road, Hsinchu 30013, Taiwan

[5] National Museum of Prehistory, No. 1, Museum Road, Taitung 95060, Taiwan

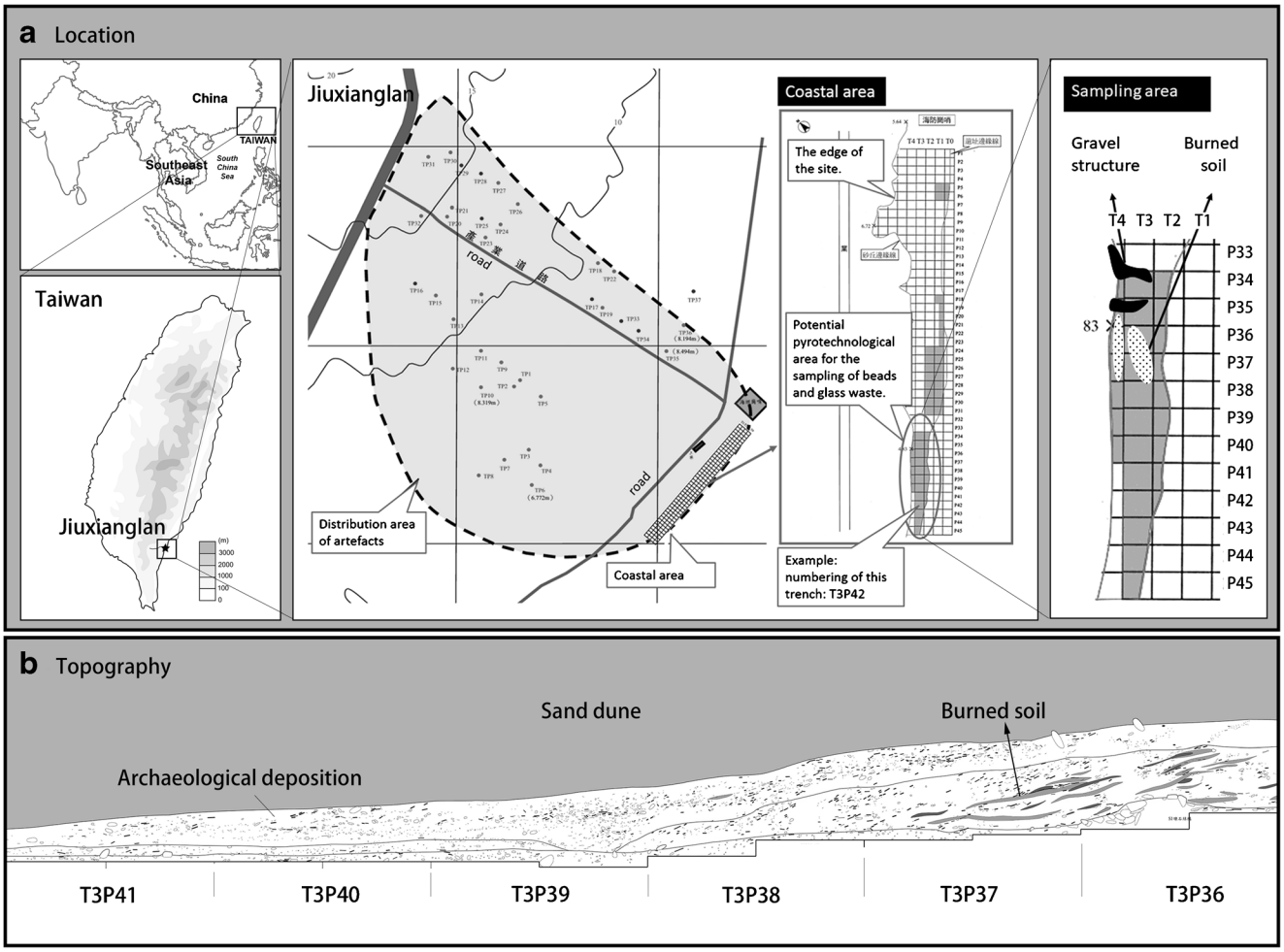

Fig. 1 **a** Map showing the location of Jiuxianglan in southeastern Taiwan and the sampling area in this research. **b** The inclined topography from the trenches T3P36 to T3P41 (the grey areas within the archaeological deposition show the inclination of burned soil)

in Iron Age Taiwan (Lee 2005b, 2007). This includes small fragments of glass rods, a mandrel encircled with a glass bead, fused glass and glass beads attached together. In addition to the glass beadmaking waste, around 2800 glass beads (intact beads or fragments) were unearthed from Jiuxianglan in the first excavation session (Lee 2005a, b; Wang 2016: 112). Except for two polychrome beads, all the remaining glass beads are monochrome, in red, orange, yellow, green, blue and black. A furnace-like circular structure built of gravel, together with burned soil areas, in proximity to the glass finds is thought to be associated with 'pyrotechnological activities' (Lee 2010: 29). This evidence together has led to speculation among Taiwan archaeologists that Jiuxianglan may be a centre of glass beadmaking and hence glass bead exchange with other cultures. To date, no detailed chemical and microstructural analyses have been done on the glass from Jiuxianglan to support this assumption. Therefore, this paper presents the first analytical study of the glass from the site, combining typology, chemical composition and microstructure to understand the relationship between the glass waste and the beads found at Jiuxianglan.

Methodology

Sample selection

Forty-four samples including 36 beads and 8 waste samples (rods, chips and chunks) were selected for analysis (Table 1). Twenty-two of the glass beads (JXL01-JXL22) were from the same trench T3P35 (Fig. 1 and Table 1; each trench is 2 m in width and 2 m in length.), where a tentative chronological sequence is proposed based on the styles of pottery handles (Lee 2005b: 159–160). T3P35 is near the gravel furnace-like structure, which partially overlaps with the trench where the glass beads were unearthed. The 22 beads were analysed to test any temporal changes in glass typology or chemical composition based on the samples from a single trench. There is no absolute dating for the trench T3P35. However, new C-14 data for nearby trenches T4P35 and T4P36 (Fig. 1) have reported in Lee (2015b: 183), suggesting an early and continuous occupation around 2150-1570BP (2 sigma calibrated results). In the southern trenches T3P37 and T3P39, the C-14 dating has shown a later chronology of 1730-1330BP and 1261-1137BP

Table 1 A list of selected samples from Jiuxianglan

Sample number	Artefact type	Location	Length (mm)	Diameter (mm)	Colour	Diaphaneity	Beadmaking method
JXL01	Bead	T3P35-SE L3	2.80	4.45	Red	Opaque	Drawn
JXL02	Bead	T3P35-SW L4	2.75	4.21	Red	Opaque	Drawn
JXL03	Bead	T3P35-NW L5	3.78	4.94	Yellow	Opaque	Drawn
JXL04	Bead	T3P35-SW L5	3.32	5.96	Light blue	Opaque	Drawn
JXL05	Bead	T3P35-NW L6	2.38	4.64	Yellow	Opaque	Drawn
JXL06	Bead	T3P35-SW L6	n/a	n/a	Light blue	Opaque	Unidentifiable
JXL07	Bead	T3P35-SW L6	3.52	4.03	Yellow	Opaque	Drawn
JXL08	Bead	T3P35-NW L7	3.32	6.56	Green	Opaque	Drawn
JXL09	Bead	T3P35-SW L7	3.61	5.84	Green	Opaque	Drawn
JXL10	Bead	T3P35-NW L8	4.96	5.12	Red	Opaque	Drawn
JXL11	Bead	T3P35-NW L8	4.19	6.65	Green	Opaque	Drawn
JXL12	Bead	T3P35-NW L9	2.62	4.37	Yellow	Opaque	Drawn
JXL13	Bead	T3P35-NW L9	4.74	4.64	Green	Opaque	Drawn
JXL14	Bead	T3P35-NW L9	3.35	4.53	Green	Opaque	Drawn
JXL15	Bead	T3P35-NW L9	3.50	4.80	Yellow	Opaque	Drawn
JXL16	Bead	T3P35-SE L12	4.05	3.73	Light blue	Opaque	Drawn
JXL17	Bead	T3P35-SE L13	3.62	4.67	Light blue	Opaque	Drawn
JXL18	Bead	T3P35-SE L13	4.91	3.35	Light blue	Opaque	Drawn
JXL19	Bead	T3P35-SE L13	3.42	4.21	Yellow	Opaque	Drawn
JXL20	Bead	T3P35-SE L13	2.15	3.43	Yellow	Opaque	Drawn
JXL21	Bead	T3P35-NW L15	3.32	3.90	Light blue	Opaque	Drawn
JXL22	Bead	T3P35-SW L15	3.85	4.44	Red	Opaque	Drawn
JXL23	Bead	T3P37-NW L14	3.48	4.42	Green	Opaque	Drawn
JXL24	Bead	T3P38-NW L6	4.06	5.26	Orange	Opaque	Drawn
JXL25	Bead	T3P38-NE L6	5.20	5.49	Orange	Opaque	Drawn
JXL26	Bead	T3P38-NW L6	3.39	n/a	Green	Opaque	Wound?
JXL27	Bead	T3P39-SW L3	2.40	2.63	Orange	Opaque	Drawn
JXL28	Bead	Surface	4.23	7.74	Light blue	Opaque	Drawn
JXL29	Bead	Surface	3.62	5.94	Light blue	Opaque	Unidentifiable
JXL30	Bead	Surface	4.18	5.19	Green	Opaque	Drawn
JXL31	Bead	Surface	3.72	4.85	Green	Opaque	Drawn
JXL32	Bead	Surface	4.75	4.52	Yellow	Opaque	Drawn
JXL33	Bead	Surface	4.12	4.88	Yellow	Opaque	Drawn
JXL34	Bead	Surface	5.39	4.89	Red	Opaque	Drawn
JXL35	Bead	Surface	3.21	5.19	Red	Opaque	Drawn
JXL38	Bead	B2	3.83	n/a	Yellow	Opaque	Drawn
JXL39	Waste	T3P38-SE L4	n/a	n/a	Light blue	Translucent	n/a
JXL41	Waste	T3P38-SE L5	n/a	n/a	Aqua	Translucent	n/a
JXL43	Waste	T3P39-SE L4	n/a	n/a	Dark blue	Opaque	n/a
JXL44	Waste	T3P39-SW L4	n/a	n/a	Light blue	Transparent	n/a
JXL46	Waste	T2P39-NW L5	n/a	n/a	Light blue	Opaque	n/a
JXL47	Waste	T3P39-SE L5	n/a	n/a	Red	Opaque	n/a
JXL48	Waste	T2P39-NW L7	n/a	n/a	Yellow	Opaque	n/a
JXL49	Waste	T2P39-NW L8	n/a	n/a	Aqua	Translucent	n/a

(2 sigma calibrated results) respectively (Lee 2015b: 183). The dating suggests the northern deposition may be of an earlier date and the southern areas may be later.

As permission was granted to sample only a limited number of beads, to increase the total sample size, 14 other beads were selected from the other trenches ($n = 5$), an Iron Age

burial ($n = 1$) and surface collections at the site ($n = 8$) (Table 1). Eight glass waste samples were selected from three trenches near the possible furnace structure to investigate the relationship between glass beads and waste and to assess the supposition that glass beads were produced at Jiuxianglan.

Optical microscopy

Optical microscopic observation was used to investigate (1) the manufacturing technique used for producing the finished glass beads sampled in this research and (2) the possible glass beadmaking method evidenced by the glass waste. Evaluation of the bead production method is based on the 'fabric' lines left on the bead surface, which may show traces resulting from the pulling of molten glass tubes (the drawn technique) or coiling of glass rods (the wound technique) (van der Sleen 1967: 24). In drawn beads, the fabric lines and elongated bubbles are parallel to the perforation axis, while in wound beads the fabric lines and bubbles encircle the perforation axis.

Chemical and microstructural analysis

The analytical parameters

Three methods were used for the chemical and microstructural analysis: scanning electron microprobe equipped with energy dispersive spectrometer (SEM-EDS) for the microstructural analysis, electron probe microanalyser (EPMA) for the quantitative analysis of major and minor elements, and laser ablation–inductively coupled plasma–mass spectrometer (LA-ICP-MS) for the trace elemental analysis. The SEM-EDS and EPMA analyses were undertaken in the EPMA Lab in the Institute of Earth Sciences, Academia Sinica, Taiwan. LA-ICP-MS analysis was carried out in the Department of Biomedical Engineering and Environmental Sciences, National Tsing Hua University, Taiwan.

All the samples selected were cut from bead fragments to get a fresh cross-section. These were then mounted in epoxy and vacuum degassed to get rid of the small bubbles. The epoxy blocks were ground and polished with diamond suspension down to 1 μm and then carbon coated for electron microprobe analysis. For LA-ICP-MS analysis, the coated carbon layer was removed prior to the analysis.

The operational parameters for SEM-EDS (JEOL FE-SEM: JSM-7100F, with Oxford EDS) are the accelerating voltage of 15 kV, the probe current of 0.1 nA and the working distance of 10 mm. The stability of beam current is routinely checked with a probe current detector.

Quantitative compositional analysis was carried out by EPMA (JEOL JXA-8500F) equipped with wavelength dispersive spectrometer (WDS). Fifteen elements are reported here, namely Si, Al, Na, K, Mg, Ca, Fe, Pb, Ba, Ti, Mn, Cu, Sn, Cl and S, reported as oxides except for Cl. The analytical parameters are, accelerating voltage of 12 kV, beam current of 6 nA and the beam diameter of 5 μm. A defocused beam was used to avoid the migration of alkalis in the glass in the bombarded area due to the beam current damage. Linear transverse EPMA analysis was used. Analytical spots were selected across the glass matrix, and voids and mineral remains in the sample were avoided. Data collected close to the bead surface were also ruled out to avoid areas of weathering or corrosion.

The LA-ICP-MS analysis was carried out using an ICP-MS spectrometer (Agilent 7500a, USA) in conjunction with a New Wave UP213 laser ablation system, combined with an Nd:YAG laser at wavelength of 213 nm. The analytical protocol follows Dussubieux et al. (2009). Single spot analysis was used with a beam diameter of 55 μm, a laser energy at around 70% of 0.2 mJ, the pulse frequency of 15 Hz and the pre-ablation time of 20s. In each sample, 4 points were analysed. The calculation of elemental concentration uses the method proposed by Gratuze (1999), and Si-29 was used as internal standard. Here, the reported elements analysed by LA-ICP-MS include Sc, V, Co, Ni, Zn, As, Rb, Sr, Y, Zr, Nb, Ag, Sb, Cs, La, Ce, Pr, Nd, Sm, Eu, Gd, Tb, Dy, Ho, Er, Tm, Yb, Lu, Hf, Th and U.

Corning A, B, C, D and NIST610, 612, 621 were used to determine the calibration curve of LA-ICP-MS analysis; for elemental concentrations not provided in the original certified value, the data from Pearce et al. (1997) were used. The limit of detection was calculated as three times the standard deviation of the measured blanks.

Precision and accuracy of the data

The standards mentioned above were also used for monitoring the precision (the repeatability of measured data) and accuracy (the conformity of the measured composition to the true composition) of the EPMA and LA-ICP-MS analysis.

The precision is evaluated by the relative standard deviation (RSD). For the EPMA results, the RSD is lower than 4% for major elements, while in minor elements the RSD is lower than 20%. In LA-ICP-MS, the RSD for most of the elements analysed is lower than 8% (except for Sb_2O_5 in Corning C and NIST 612, with RSD ~ 29 and 16%, respectively).

In terms of the accuracy, in EPMA the relative accuracy error of major elements varies from − 5.3 to 3.0%, and the measured value of K_2O is always slightly lower than that reported in the Corning standards. As for minor elements, the relative accuracy is generally between − 60.4 and 58.7%. The measured value of MnO in Corning C shows a large relative accuracy error of − 96.8% (with a measured value of 0.03%) compared to that reported in Vicenzi et al. (2002, 0.82%). In fact, varied values of MnO in Corning C were reported, and a low MnO content of around 0.001% is also

reported in Dussubieux et al. (2009) and Wagner et al. (2012). The relevant discussion can be found in Wagner et al. (2012).

In LA-ICP-MS, the relative accuracy error for the trace elements it is between 33 and −30%. The relative accuracy error of Sb_2O_5 is particularly high in Corning C, which may be due to the overestimation of the recommended value in Brill (1999: 544). A relatively low value of Sb_2O_5 is reported in Dussubieux et al. (2009) (0.00014%) and Wagner et al. (2012) (0.0001%), and in this research the Sb_2O_5 is measured as 0.0006% in Corning C.

Results

Optical microscopic observation

The optical microscopic investigation revealed that 33 of the 36 beads are probably drawn. Figure 2 shows some bead samples with evidence of the drawn method where the parallel fabric lines, elongated bubbles and voids can be seen clearly on the surface. The manufacturing method of one green bead, JXL26, is hard to determine simply through the exterior surface, but further examination on the perforation and interior body reveals a few encircling fabric lines, and therefore may suggest the use of the wound method. The manufacturing method for the remaining two blue beads (JXL06 and JXL29, Fig. 2) could not be determined through microscopic observation.

In the red beads, blackish streaks are often noticed, and in the green beads, yellowish streaks can be seen. The optical microscopic examination clearly indicates that these blackish or yellowish streaks are not intentionally added on the bead surface for decoration, as they can also be observed from the interior body through the fragmented surface and are therefore a result of the drawn manufacturing method used (JXL01 and JXL11, Fig. 2). In the green bead, this is probably the result of an uneven distribution of the colourant used, based on the chemical and microstructural analysis (Wang 2016: 173–175). In terms of the red heterogeneities, no distinct chemical and microstructural differences can be seen with SEM-EDS despite these being visibly distinct, suggesting that more scientific analysis, and possibly experimentation, is required to understand the mechanisms between the red and blackish areas.

In terms of the glass waste, it can be seen from Fig. 2 that the shapes of the waste do not suggest the use of the technique, described by Francis (1990), used for producing drawn beads in the Indo-Pacific region. None of the waste resembles specific artefacts or features of this type of production, for example, the ‘horns’, the ‘pulled tubes’ and the ‘caught knots’

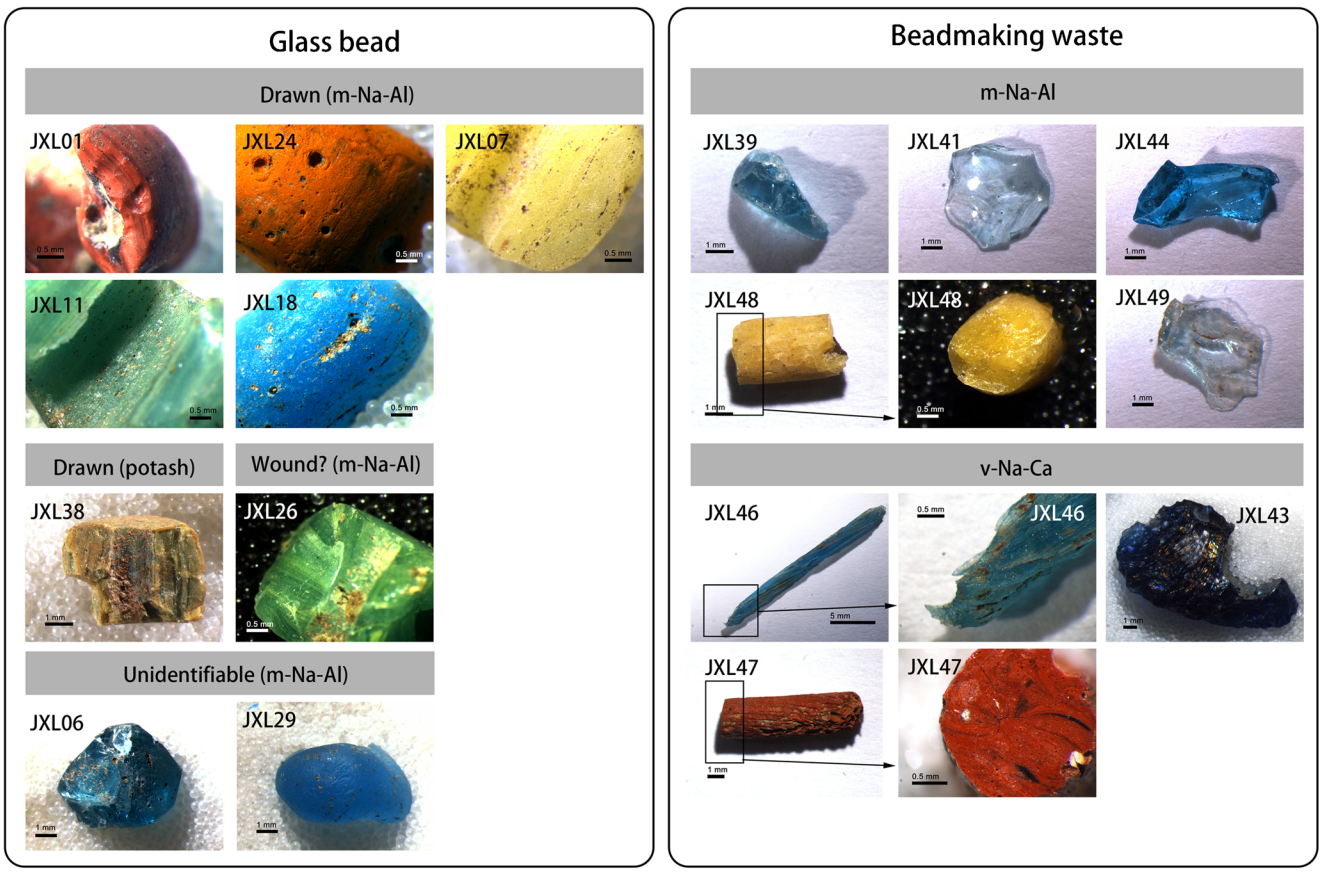

Fig. 2 Optical microscopic images of glass beads and waste from Jiuxianglan

suggested by Peter Francis as indicative evidence of the drawn method (Francis 1990). Similarly, there are no remains of glass tubes found at Jiuxianglan which would be expected if the drawn method was used. Figure 2 shows JXL46, JXL47 and JXL48 are all glass rods rather than tubes. The image of JXL46 further shows the stretched pulled-off end of the glass rod. This lack of waste indicative of drawn beads and the absence of tubes, along with the presence of glass rods together with the bead encircling the tip of a mandrel (shown in Lee 2005a), suggests it is more likely that the *wound* method rather than drawn method was used for bead production at Jiuxianglan. Therefore, the identification of the wound method from glass waste shows an inconsistency with the examined finished glass beads, which were made using the drawn method.

Chemical composition and microstructure

In the 44 glass samples analysed, 40 are mineral-soda-alumina (m-Na-Al) glass (Fig. 3, Tables 2 and 3), with Na_2O greater than 15 wt%, Al_2O_3 between 6 and 15 wt% and MgO less than 2 wt% in the base composition. Three samples are soda plant ash glass (v-Na-Ca glass, v=vegetal), having Na_2O at a similar level to the m-Na-Al glass, but Al_2O_3 contents are less than 5 wt% and MgO between 3 and 6 wt%. There is only one potash glass identified in this research, with K_2O 15 wt%, Al_2O_3 2 wt% and MgO less than 1 wt% (see Dussubieux and Gratuze (2010) and Wang and Jackson (2014) for a review of these compositions).

All but one of the glass beads analysed here have an m-Na-Al composition ($n = 35$, Fig. 3). The other glass bead is a potash glass. All the samples selected from the single trench (JXL01-JXL22) are m-Na-Al glass with an extremely consistent composition, the only significant compositional differences being the added colourants. As for the glass waste, five

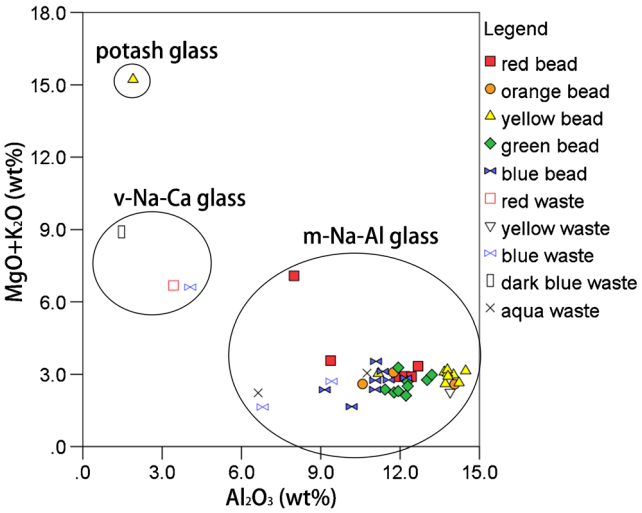

Fig. 3 The chemical groups of glass analysed in this research, showing the relative proportions of m-Na-Al glass, v-Na-Ca glass and potash glass

samples are m-Na-Al glass and three are v-Na-Ca glass. This contrasts with the beads analysed where there are no examples of v-Na-Ca glass. Moreover, the chemical composition and/or microstructure of m-Na-Al glass *waste* also does not always show similarities to the m-Na-Al glass *beads*; these anomalies are discussed below.

Yellow glass beads and waste

Further investigation of the yellow m-Na-Al glass beads ($n = 9$) and waste ($n = 1$), has shown that all the yellow glass beads (excluding JXL20) have similar levels of CaO (~2.5 wt%), Ba (~0.25 wt%) and Sr (~700 ppm), but the one yellow m-Na-Al glass waste fragment (JXL48) has lower concentrations of CaO (1.7 wt%), Ba (0.13 wt%) and Sr (400 ppm) (Fig. 4). JXL20 is regarded as an outlier here, as the Ba and Sr concentrations are much lower than other yellow bead samples (Table 2).

The yellow glasses have elevated level of Sr. Although this may suggest a marine carbonate source (Freestone et al. 2003), the relationships between the CaO, Sr and Ba in the yellow glass suggest marine carbonates may not be the dominant contributor of the elevated level of Sr seen here. The microstructural analysis on the m-Na-Al glass from Jiuxianglan has suggested that the granitic sand used in the glass production is rich in plagioclase, which may introduce a few percent of CaO and a few hundred ppm of Ba and Sr to the bulk composition of glass (Wang et al. submitted). Thus the increased concentrations of Sr may also derive from the plagioclase in the sand. Moreover, the CaO concentration at less than 3 wt% does not suggest an additional source of crushed shell was introduced into the primary glass during production. However, despite this the Ba and Sr contents in the yellow glass *beads* from Jiuxianglan are higher than the average level of Ba (420–840 ppm) and Sr (100–400 ppm) in granitic rocks (Mielke 1979), and therefore may indicate some other additional sources of Ba and Sr in the yellow glass beads as this does not fully explain this high concentration of these elements.

It is tentatively suggested that some of the Ba, and possibly Sr, in the yellow glass beads may be introduced as impurities of a Pb-containing ingredient used as a colourant, as these yellow glass beads are coloured by lead tin oxide, and lead ores such as galena (PbS) often precipitates with barite ($BaSO_4$) and/or celestine ($SrSO_4$) (Wang 2016: 145–148). In the yellow glass beads, a PbO/Ba ratio of less than 18 is found, while in the yellow glass waste the PbO/Ba ratio is 45. This may suggest that different raw materials, bead origins or recipes specifically related to the colouring of the beads were used in the production of yellow glass beads and the waste found at Jiuxianglan, although all were coloured and opacified by lead tin oxide.

Further investigation on the PbO-SnO_2 relationship in this material indicates different mixes or recipes of colourants

Table 2 Chemical composition of samples from Jiuxianglan (wt%) (major and minor elements analysed by EPMA). *n* = number of analyses

	Colour	Artefact type	*n*	Compo	SiO_2 (%)	Al_2O_3 (%)	Na_2O (%)	K_2O (%)	MgO (%)	CaO (%)	FeO (%)	MnO (%)	CuO (%)	SnO_2 (%)	PbO (%)	Cl (%)	SO_3 (%)	Ti (%)	Ba (%)
JXL01	Red	Bead	48	m-Na-Al	59.29	11.41	18.49	2.24	0.55	3.15	1.10	0.07	1.17	0.06	0.86	1.01	0.15	0.35	0.16
JXL02	Red	Bead	44	m-Na-Al	59.44	11.72	18.55	2.34	0.47	2.57	1.15	0.05	1.14	0.06	0.78	1.07	0.15	0.37	0.14
JXL03	Yellow	Bead	39	m-Na-Al	57.02	13.27	18.08	2.49	0.33	2.37	1.07	0.04	0.08	0.14	3.06	0.91	0.13	0.32	0.23
JXL04	Blue	Bead	29	m-Na-Al	61.83	10.65	18.38	3.29	0.11	1.19	0.62	0.05	1.05	0.00	0.30	0.86	0.18	0.28	0.12
JXL05	Yellow	Bead	35	m-Na-Al	55.65	13.23	21.19	2.58	0.42	2.58	1.12	0.04	0.09	0.04	1.22	1.12	0.24	0.40	0.24
JXL06	Blue	Bead	44	m-Na-Al	59.33	8.87	21.15	1.82	0.48	4.09	1.24	0.06	0.52	0.01	0.05	0.61	0.42	0.31	0.10
JXL07	Yellow	Bead	46	m-Na-Al	56.45	12.96	19.09	2.16	0.30	2.35	1.23	0.06	0.05	0.11	2.31	1.09	0.14	0.47	0.25
JXL08	Green	Bead	55	m-Na-Al	60.92	11.22	16.63	2.89	0.20	1.38	0.79	0.04	0.52	0.10	3.11	0.99	0.07	0.26	0.10
JXL09	Green	Bead	36	m-Na-Al	57.31	10.78	17.94	1.72	0.35	2.30	1.21	0.04	0.52	0.38	4.15	1.05	0.29	0.38	0.14
JXL10	Red	Bead	32	m-Na-Al	59.27	8.90	19.40	1.95	1.45	2.09	1.86	0.15	1.61	0.13	0.34	0.97	0.29	0.43	0.10
JXL11	Green	Bead	32	m-Na-Al	59.20	11.32	15.84	2.14	0.35	2.20	1.14	0.07	0.72	0.22	3.95	0.88	0.08	0.35	0.16
JXL12	Yellow	Bead	27	m-Na-Al	55.99	12.87	18.03	2.45	0.40	2.29	1.34	0.03	0.07	0.31	3.08	0.95	0.10	0.41	0.21
JXL13	Green	Bead	38	m-Na-Al	57.93	12.20	17.08	2.23	0.37	2.54	1.34	0.07	0.53	0.31	3.38	0.86	0.11	0.39	0.21
JXL14	Green	Bead	26	m-Na-Al	58.18	11.27	16.39	1.91	0.39	2.31	1.28	0.04	0.88	0.33	4.01	0.92	0.09	0.36	0.14
JXL15	Yellow	Bead	32	m-Na-Al	56.04	12.99	18.56	2.58	0.42	2.34	1.27	0.05	0.06	0.09	2.37	0.98	0.11	0.38	0.25
JXL16	Blue	Bead	39	m-Na-Al	62.28	10.46	16.33	2.30	0.30	1.91	0.95	0.05	1.16	0.11	1.35	0.97	0.08	0.27	0.12
JXL17	Blue	Bead	48	m-Na-Al	63.17	10.62	17.20	2.06	0.22	1.77	1.07	0.13	0.93	0.05	0.23	1.06	0.06	0.46	0.17
JXL18	Blue	Bead	43	m-Na-Al	62.08	10.94	17.93	2.74	0.27	1.48	0.98	0.04	1.03	0.01	0.04	1.05	0.06	0.32	0.10
JXL19	Yellow	Bead	36	m-Na-Al	55.87	12.80	17.91	2.41	0.31	2.26	1.17	0.04	0.07	0.09	4.03	0.98	0.12	0.42	0.23
JXL20	Yellow	Bead	47	m-Na-Al	62.48	10.65	17.13	2.64	0.25	1.35	0.73	0.03	0.05	0.05	2.26	1.17	0.04	0.31	0.12
JXL21	Blue	Bead	32	m-Na-Al	60.39	11.86	19.54	2.55	0.22	1.61	0.84	0.03	1.33	0.15	0.19	1.22	0.08	0.28	0.14
JXL22	Red	Bead	45	m-Na-Al	58.59	12.07	17.49	2.59	0.59	2.58	1.27	0.06	1.23	0.06	0.61	0.97	0.12	0.41	0.17
JXL23	Green	Bead	33	m-Na-Al	57.18	12.01	15.86	2.43	0.28	2.15	1.10	0.03	1.36	0.43	5.62	0.96	0.08	0.34	0.20
JXL24	Orange	Bead	28	m-Na-Al	52.73	12.55	15.52	1.47	0.85	3.62	2.55	0.03	7.45	1.24	1.55	0.49	0.26	0.33	0.09
JXL25	Orange	Bead	34	m-Na-Al	57.38	9.63	16.62	1.50	0.87	3.05	1.94	0.05	4.75	0.47	1.43	0.95	0.21	0.25	0.09
JXL26	Green	Bead	42	m-Na-Al	60.31	10.70	17.07	1.92	0.30	2.16	1.14	0.04	1.08	0.13	2.70	1.04	0.10	0.38	0.15
JXL27	Orange	Bead	58	m-Na-Al	58.99	10.81	14.48	2.04	0.79	3.18	1.70	0.03	5.20	0.39	0.90	0.84	0.28	0.20	0.10
JXL28	Blue	Bead	53	m-Na-Al	63.45	11.28	17.52	2.48	0.23	1.69	0.83	0.05	0.86	0.03	0.26	1.07	0.09	0.25	0.11
JXL29	Blue	Bead	36	m-Na-Al	62.78	9.86	19.89	1.38	0.23	1.97	0.79	0.07	0.87	0.05	0.21	1.33	0.11	0.29	0.09
JXL30	Green	Bead	47	m-Na-Al	60.86	11.56	16.59	1.62	0.38	2.38	1.19	0.07	0.69	0.11	2.11	1.04	0.10	0.39	0.16
JXL31	Green	Bead	32	m-Na-Al	61.40	11.13	15.33	1.81	0.33	2.23	1.08	0.09	0.71	0.11	2.70	0.88	0.09	0.35	0.15
JXL32	Yellow	Bead	37	m-Na-Al	56.34	13.37	18.42	2.18	0.31	2.22	1.12	0.03	0.05	0.20	2.64	1.06	0.12	0.40	0.24
JXL33	Yellow	Bead	47	m-Na-Al	57.83	13.89	17.50	2.63	0.39	2.45	1.28	0.04	0.05	0.08	1.66	0.98	0.08	0.45	0.22
JXL34	Red	Bead	15	m-Na-Al	61.88	7.64	14.41	4.73	2.04	3.61	1.24	0.10	0.94	0.06	0.33	0.80	0.06	0.21	0.16
JXL35	Red	Bead	49	m-Na-Al	61.53	12.03	16.77	2.36	0.44	2.37	1.25	0.05	1.29	0.15	0.34	0.92	0.10	0.40	0.20

Table 2 (continued)

	Colour	Artefact type	*n*	Compo	SiO_2 (%)	Al_2O_3 (%)	Na_2O (%)	K_2O (%)	MgO (%)	CaO (%)	FeO (%)	MnO (%)	CuO (%)	SnO_2 (%)	PbO (%)	Cl (%)	SO_3 (%)	Ti (%)	Ba (%)
JXL38	Yellow	Bead	27	potash	73.43	1.72	0.40	13.64	0.16	0.90	0.41	0.20	1.85	0.10	3.55	0.13	0.06	0.03	0.07
JXL39	Blue	Waste	45	m-Na-Al	63.08	9.19	19.81	2.32	0.32	1.88	1.04	0.04	0.31	0.01	0.09	0.42	0.37	0.32	0.08
JXL41	Aqua	Waste	39	m-Na-Al	67.60	6.45	18.06	1.78	0.39	1.83	1.21	0.05	0.21	0.01	0.03	0.46	0.38	0.29	0.11
JXL43	Dark blue	Waste	58	v-Na-Ca	64.03	1.40	15.84	2.79	5.80	5.29	1.19	1.57	0.24	0.00	0.02	0.59	0.28	0.06	0.04
JXL44	Blue	Waste	33	m-Na-Al	66.90	6.57	18.03	1.34	0.24	2.37	1.14	0.07	0.82	0.06	0.06	0.51	0.33	0.36	0.10
JXL46	Blue	Waste	48	v-Na-Ca	60.26	3.93	19.78	2.66	3.73	5.47	0.83	0.03	0.98	0.00	0.04	1.17	0.21	0.09	0.05
JXL47	Red	Waste	40	v-Na-Ca	59.33	3.28	16.46	2.50	3.89	8.52	1.65	0.48	1.26	0.06	0.34	0.59	0.33	0.11	0.06
JXL48	Yellow	Waste	36	m-Na-Al	54.27	12.62	19.51	1.94	0.12	1.75	0.67	0.03	0.06	0.62	5.83	0.88	0.30	0.27	0.13
JXL49	Aqua	Waste	40	m-Na-Al	62.26	10.53	19.49	2.70	0.28	1.91	0.73	0.04	0.20	0.00	0.02	0.40	0.22	0.30	0.13

were used in the glass beads and glass waste. The yellow glass beads contain less than 4 wt% PbO and 0.4 wt% SnO_2 (with a variable PbO/SnO_2 ratio between 10 and 45), while the yellow glass waste has greater PbO of around 6 wt% and SnO_2 of 0.6 wt% (Fig. 5). It is therefore likely that the yellow glass beads and waste from Jiuxianglan were not coloured using the same source or mixture of colourant. This further indicates that the yellow glass beads from Jiuxianglan are not locally produced and the glass waste analysed in this research is unrelated to the beads.

One yellow glass bead is made of potash glass. Microstructural investigation has revealed that this glass may have been a green glass originally, and the outer yellowish colour is a result of weathering (Wang et al. submitted). The lack of potash glass waste means that it is not possible to investigate whether this bead may have been locally produced at Jiuxianglan.

Light blue glass beads and waste and dark blue glass waste

The light blue glass is coloured by CuO. All the light blue glass beads ($n = 8$) are m-Na-Al glass, 2 light blue glass waste fragments are m-Na-Al glass and 1 light blue waste fragment is v-Na-Ca glass. The dark blue waste has a v-Na-Ca composition, coloured by cobalt (770 ppm) and shows a homogeneous matrix. Unfortunately, permission was not given to analyse any dark blue glass beads in this research.

The chemical composition of the m-Na-Al glass does not show significant differences between light blue glass beads and waste. However, it is noteworthy that the two light blue m-Na-Al glass *waste* fragments have a different microstructure to the light blue beads. Although the matrix of the light blue glass bead is more homogeneous compared to other bead colours, the light blue *beads* contain bubbles, un-melted minerals (such as silica, feldspar and zircon) and sometimes exhibit an uneven chemical distribution of glass matrix (localised inhomogeneity) (Fig. 6a, b). In contrast, the glass matrix of the m-Na-Al glass *waste* is relatively homogeneous with the absence of bubbles and almost no un-melted silica or feldspar relics (Fig. 6c, d). Figure 2 also clearly shows that the light blue m-Na-Al glass waste (JXL39 and JXL44) is visibly transparent, but the beads are opaque. One light blue glass waste fragment (JXL46) has a v-Na-Ca composition, but no beads of v-Na-Ca glass were found in this analysis. This light blue glass waste fragment shows a homogeneous matrix without any obvious mineral remains. These factors taken together may suggest the light blue beads (all m-Na-Al glass) and waste (m-Na-Al or v-Na-Ca composition) from Jiuxianglan are not related.

Aqua glass waste

Two aqua glass waste fragments were analysed, and both are m-Na-Al glass. The two aqua glasses reveal slightly different

Table 3 Chemical composition of samples from Jiuxianglan (ppm) (minor and trace elements analysed by LA-ICP-MS). *n* = number of analyses, <LLD=not detected, samples with no data indicate the sample was not analysed

	Colour	Artefact type	*n*	Compo	Sc (ppm)	V (ppm)	Co (ppm)	Ni (ppm)	Zn (ppm)	As (ppm)	Rb (ppm)	Sr (ppm)	Y (ppm)	Zr (ppm)	Nb (ppm)	Ag (ppm)	Sb (ppm)	Cs (ppm)	La (ppm)
JXL01	Red	Bead	4	m-Na-Al															
JXL02	Red	Bead	4	m-Na-Al	2.0	51.2	<LLD	<LLD	10.6	<LLD	27.0	511.8	6.7	390.9	5.0	21.7	13.3	<LLD	19.9
JXL03	Yellow	Bead	4	m-Na-Al	2.2	52.5	<LLD	<LLD	<LLD	<LLD	31.3	664.6	6.1	267.0	3.7	6.4	1.6	<LLD	21.0
JXL04	Blue	Bead	4	m-Na-Al	2.0	70.5	2.52	4.5	29.1	14.6	75.7	299.5	5.4	362.8	10.6	19.6	11.4	0.7	10.8
JXL05	Yellow	Bead	4	m-Na-Al	<LLD	52.2	4.52	27.8	11.2	4.7	37.3	713.5	6.8	540.7	5.0	5.1	1.5	0.7	26.2
JXL06	Blue	Bead	4	m-Na-Al	2.5	77.4	<LLD	<LLD	<LLD	<LLD	36.2	335.5	12.8	390.7	3.4	0.7	3.5	<LLD	27.6
JXL07	Yellow	Bead	4	m-Na-Al	2.8	58.8	<LLD	<LLD	<LLD	<LLD	29.8	734.0	7.0	388.7	5.4	5.0	5.5	<LLD	26.4
JXL08	Green	Bead	4	m-Na-Al	2.5	28.4	<LLD	<LLD	<LLD	<LLD	56.8	298.1	6.8	320.4	7.3	13.0	12.5	<LLD	11.7
JXL09	Green	Bead																	
JXL10	Red	Bead	4	m-Na-Al	6.6	67.5	19.61	54.8	119.5	33.7	50.7	286.2	14.6	451.6	6.7	42.2	10.5	0.6	38.0
JXL11	Green	Bead	4	m-Na-Al	6.3	52.8	8.69	4.8	44.0	14.2	37.9	539.6	9.1	477.8	6.4	13.4	8.4	0.7	23.5
JXL12	Yellow	Bead	4	m-Na-Al	4.6	56.8	4.67	6.4	25.8	7.1	46.4	735.3	7.7	256.4	6.4	3.4	0.6	0.1	32.3
JXL13	Green	Bead	4	m-Na-Al	<LLD	53.4	11.36	40.3	61.6	13.7	34.5	629.0	8.8	514.6	5.4	8.4	4.5	0.7	27.4
JXL14	Green	Bead	4	m-Na-Al	2.8	52.5	6.84	12.4	40.8	17.4	34.7	649.1	10.6	501.7	6.8	22.2	11.3	0.2	27.0
JXL15	Yellow	Bead	4	m-Na-Al	3.5	58.1	3.24	6.8	18.3	8.2	44.5	765.2	6.9	303.2	6.2	4.6	0.4	0.6	29.2
JXL16	Blue	Bead	4	m-Na-Al	0.9	50.2	4.52	7.1	63.8	15.3	48.3	402.1	8.2	442.1	6.3	32.4	8.2	0.6	17.9
JXL17	Blue	Bead	4	m-Na-Al	5.6	39.0	12.42	4.4	49.8	14.0	34.0	403.3	10.5	653.8	8.1	5.8	8.1	0.4	19.2
JXL18	Blue	Bead	4	m-Na-Al	2.6	44.6	3.63	4.6	45.7	14.4	70.2	254.5	12.6	322.2	10.8	3.7	7.7	0.5	17.5
JXL19	Yellow	Bead	4	m-Na-Al	4.9	51.7	2.50	<LLD	21.2	9.7	39.2	731.8	5.9	273.8	5.8	2.1	2.4	0.9	24.9
JXL20	Yellow	Bead	4	m-Na-Al	<LLD	38.1	2.62	16.4	14.3	3.6	51.5	273.2	6.1	274.4	11.6	27.3	3.3	0.5	12.8
JXL21	Blue	Bead	4	m-Na-Al	1.4	41.0	<LLD	<LLD	<LLD	<LLD	43.6	256.7	8.3	230.8	6.3	1.2	11.5	<LLD	12.3
JXL22	Red	Bead	4	m-Na-Al	6.4	57.2	4.30	3.8	61.7	13.0	46.3	654.3	9.9	529.3	6.6	17.3	15.1	0.9	27.6
JXL23	Green	Bead	4	m-Na-Al	2.6	31.4	<LLD	<LLD	<LLD	<LLD	37.1	502.5	6.2	165.7	4.5	74.4	3.7	<LLD	19.2
JXL24	Orange	Bead	4	m-Na-Al	5.3	71.0	21.69	13.6	1773.6	297.4	28.1	421.3	8.1	249.4	3.5	48.4	50.3	<LLD	28.1
JXL25	Orange	Bead	4	m-Na-Al	5.1	100.8	10.65	57.4	1103.3	92.6	36.1	352.5	12.0	156.2	3.3	44.9	91.6	0.5	25.5
JXL26	Green	Bead	4	m-Na-Al	<LLD	47.5	5.41	24.4	38.7	10.5	26.3	533.5	9.7	555.9	5.9	33.5	10.0	0.4	24.9
JXL27	Orange	Bead	4	m-Na-Al	3.4	101.0	10.89	71.0	735.0	178.2	36.2	447.1	10.1	221.8	3.3	36.8	120.1	0.8	26.6
JXL28	Blue	Bead	4	m-Na-Al	<LLD	43.3	6.11	36.7	17.3	6.2	35.0	320.3	11.2	351.2	6.5	12.5	7.6	0.7	19.4
JXL29	Blue	Bead	4	m-Na-Al	<LLD	50.8	3.84	30.1	46.5	10.8	16.4	372.2	12.3	519.3	4.8	10.3	8.2	0.6	22.0
JXL30	Green	Bead	4	m-Na-Al	<LLD	49.8	10.87	35.4	113.4	11.0	26.7	521.8	11.2	393.2	6.5	15.2	5.2	0.8	26.1
JXL31	Green	Bead	4	m-Na-Al	2.9	49.1	12.80	10.4	18.8	12.8	32.3	523.9	10.8	388.9	5.6	8.8	7.8	1.4	25.4
JXL32	Yellow	Bead	4	m-Na-Al	4.8	56.3	2.78	8.7	22.7	8.1	34.0	801.3	7.6	297.3	6.0	3.8	1.2	0.4	26.7
JXL33	Yellow	Bead	4	m-Na-Al	<LLD	43.6	3.80	15.9	20.2	2.2	37.0	693.2	7.3	178.4	6.7	1.2	2.2	0.9	27.3
JXL34	Red	Bead	4	m-Na-Al	3.5	39.9	9.20	19.8	172.3	22.9	102.3	497.8	12.3	359.3	5.0	7.2	12.9	0.6	21.2
JXL35	Red	Bead	4	m-Na-Al	<LLD	52.6	10.92	70.5	68.2	27.1	36.7	640.5	8.1	593.0	5.8	14.6	18.5	1.0	30.4

Table 3 (continued)

JXL38	Yellow	Bead	4	potash	3.1	12.2	15.80	5.9	20.1	146.1	405.5	26.6	4.1	38.2	1.0	68.5	184.5	2.2	9.3	
JXL39	Blue	Waste	4	m-Na-Al	0.6	64.6	4.15	15.7	13.8	4.3	64.3	261.6	7.9	517.8	6.6	3.6	4.0	0.6	64.2	
JXL41	Aqua	Waste	4	m-Na-Al	4.2	93.1	3.52	3.5	13.6	9.4	44.0	231.1	7.2	685.8	6.0	1.3	2.3	0.4	38.7	
JXL43	Dark blue	Waste	4	v-Na-Ca	<LLD	15.6	773.48	60.6	1161.4	11.3	12.2	466.8	4.6	133.6	1.3	0.9	2.7	0.4	8.3	
JXL44	Blue	Waste																		
JXL46	Blue	Waste	4	v-Na-Ca	4.6	10.6	6.22	15.2	32.1	22.3	23.3	417.2	8.8	58.7	3.5	1.0	8.6	0.9	29.2	
JXL47	Red	Waste	4	v-Na-Ca	4.7	18.5	5.31	53.2	51.9	31.2	16.7	456.0	5.8	63.7	2.2	8.4	114.6	0.4	9.0	
JXL48	Yellow	Waste	4	m-Na-Al	3.2	28.6	2.88	5.1	20.3	5.7	22.2	434.3	6.0	243.4	2.5	10.8	1.7	0.6	10.8	
JXL49	Aqua	Waste	4	m-Na-Al	2.6	46.2	2.25	5.3	17.0	5.9	84.3	341.3	6.8	412.9	6.9	1.6	0.7	0.9	73.6	

	Colour	Artefact type	*n*	Compo	Ce (ppm)	Pr (ppm)	Nd (ppm)	Sm (ppm)	Eu (ppm)	Gd (ppm)	Tb (ppm)	Dy (ppm)	Ho (ppm)	Er (ppm)	Tm (ppm)	Yb (ppm)	Lu (ppm)	Hf (ppm)	Th (ppm)	U (ppm)
JXL01	Red	Bead																		
JXL02	Red	Bead	4	m-Na-Al	33.7	2.9	10.7	1.2	0.3	1.6	0.1	0.4	0.1	0.2	<LLD	<LLD	<LLD	6.6	4.9	8.0
JXL03	Yellow	Bead	4	m-Na-Al	32.7	2.8	10.2	0.2	0.4	1.4	0.1	0.5	<LLD	<LLD	<LLD	<LLD	<LLD	5.0	3.4	4.3
JXL04	Blue	Bead	4	m-Na-Al	20.6	1.8	5.4	1.1	0.5	1.6	0.2	<LLD	0.2	0.6	0.4	2.0	0.2	9.1	3.7	3.7
JXL05	Yellow	Bead	4	m-Na-Al	35.6	3.3	11.4	2.2	0.7	1.8	0.5	1.6	0.3	1.7	0.4	<LLD	0.4	12.7	6.8	3.4
JXL06	Blue	Bead	4	m-Na-Al	36.8	3.7	14.6	1.7	0.4	0.5	0.2	1.7	0.5	<LLD	0.3	<LLD	<LLD	6.8	4.6	4.3
JXL07	Yellow	Bead	4	m-Na-Al	45.7	3.6	11.0	1.0	0.1	1.3	0.1	<LLD	0.0	<LLD	<LLD	<LLD	<LLD	6.2	5.9	20.3
JXL08	Green	Bead	4	m-Na-Al	22.8	1.5	4.3	1.8	0.1	1.0	0.1	<LLD	0.0	<LLD	<LLD	<LLD	<LLD	4.9	2.9	16.1
JXL09	Green	Bead																		
JXL10	Red	Bead	4	m-Na-Al	48.7	6.0	25.5	3.6	0.8	4.7	0.5	2.5	0.4	1.0	0.4	1.7	0.6	9.9	6.9	5.0
JXL11	Green	Bead	4	m-Na-Al	38.1	3.3	14.5	2.6	1.2	3.0	0.3	2.1	0.3	0.8	0.1	<LLD	0.3	12.2	5.0	9.1
JXL12	Yellow	Bead	4	m-Na-Al	45.2	4.2	16.5	3.0	0.9	2.7	0.4	2.2	0.3	1.0	0.4	<LLD	0.2	7.0	6.6	4.0
JXL13	Green	Bead	4	m-Na-Al	44.7	3.7	17.3	3.5	1.1	3.5	0.7	2.9	0.6	1.6	0.2	<LLD	0.2	12.1	7.8	7.8
JXL14	Green	Bead	4	m-Na-Al	43.5	3.8	16.3	2.8	1.6	3.3	0.6	2.4	0.3	1.3	0.6	1.8	0.3	12.3	5.9	7.8
JXL15	Yellow	Bead	4	m-Na-Al	42.2	4.0	17.2	2.8	1.4	2.4	0.4	2.4	0.4	0.5	0.4	1.7	0.4	5.8	5.2	3.8
JXL16	Blue	Bead	4	m-Na-Al	32.6	3.0	12.0	1.3	0.8	2.8	0.3	1.0	0.3	1.1	<LLD	<LLD	0.3	11.2	5.0	9.4
JXL17	Blue	Bead	4	m-Na-Al	36.3	3.2	15.2	2.4	0.9	2.2	0.5	2.2	0.2	1.1	0.4	1.5	0.3	15.4	6.2	6.9
JXL18	Blue	Bead	4	m-Na-Al	38.3	3.0	12.2	1.6	0.8	3.0	0.5	2.6	0.5	1.6	<LLD	2.9	0.4	7.2	5.7	16.4
JXL19	Yellow	Bead	4	m-Na-Al	40.1	3.9	16.4	1.3	1.0	2.5	0.5	1.7	0.3	0.7	0.5	<LLD	0.2	7.6	6.1	11.0
JXL20	Yellow	Bead	4	m-Na-Al	30.6	1.7	8.9	2.9	0.4	2.1	0.4	3.3	<LLD	1.6	0.3	<LLD	0.3	8.5	5.4	12.2
JXL21	Blue	Bead	4	m-Na-Al	32.2	1.8	6.2	1.3	0.3	1.3	0.2	0.4	0.2	<LLD	<LLD	0.2	<LLD	3.9	4.7	32.9
JXL22	Red	Bead	4	m-Na-Al	42.9	4.3	16.4	2.6	1.3	3.1	0.3	1.7	0.2	1.1	0.3	2.0	0.3	13.0	6.4	7.8
JXL23	Green	Bead	4	m-Na-Al	32.6	2.5	8.2	1.3	0.1	1.6	0.1	0.7	<LLD	<LLD	<LLD	<LLD	<LLD	2.8	4.8	11.1
JXL24	Orange	Bead	4	m-Na-Al	43.4	4.1	13.9	1.8	0.3	1.2	0.1	0.6	0.0	<LLD	<LLD	<LLD	<LLD	4.0	3.8	7.0
JXL25	Orange	Bead	4	m-Na-Al	33.4	4.0	18.8	1.9	0.9	3.7	0.4	2.0	0.5	1.2	0.3	2.2	0.4	4.5	8.6	10.3
JXL26	Green	Bead	4	m-Na-Al	42.9	3.9	16.1	3.2	0.8	2.3	0.4	2.5	0.4	1.4	0.2	<LLD	0.4	13.6	7.5	13.5
JXL27	Orange	Bead	4	m-Na-Al	34.4	4.2	16.7	2.8	0.6	2.9	0.5	2.0	0.3	0.9	0.3	<LLD	0.2	5.8	10.9	8.2
JXL28	Blue	Bead	4	m-Na-Al	34.7	3.4	13.1	4.6	0.5	1.0	0.6	2.8	0.7	2.0	0.1	<LLD	0.5	7.3	6.4	18.7
JXL29	Blue	Bead	4	m-Na-Al	39.4	3.5	16.4	2.4	0.9	3.3	0.5	2.8	0.5	1.7	0.3	<LLD	0.3	12.2	7.2	9.0
JXL30	Green	Bead	4	m-Na-Al	45.6	4.4	19.0	4.0	1.2	2.8	0.8	2.9	0.6	1.6	0.3	<LLD	0.4	8.9	7.0	8.2
JXL31	Green	Bead	4	m-Na-Al	41.6	4.0	14.4	3.6	0.5	3.6	0.4	2.5	0.4	0.8	<LLD	2.3	0.2	9.7	4.8	6.0
JXL32	Yellow	Bead	4	m-Na-Al	46.1	3.8	16.5	2.6	1.3	2.5	0.3	1.3	0.3	1.5	0.4	2.3	0.2	6.1	5.3	14.9
JXL33	Yellow	Bead	4	m-Na-Al	37.7	3.8	13.7	2.9	0.6	1.1	0.6	2.1	0.3	1.2	0.1	<LLD	0.3	4.7	5.5	6.3
JXL34	Red	Bead	4	m-Na-Al	41.0	3.6	14.6	2.1	0.8	4.4	0.4	3.3	0.4	1.7	0.4	2.5	0.4	8.3	6.0	13.8

Table 3 (continued)

JXL35	Red	Bead	4	m-Na-Al	49.0	4.1	17.2	2.4	1.1	2.6	0.4	2.2	0.3	1.2	0.2	<LLD	0.6	12.5	9.0	10.7
JXL38	Yellow	Bead	4	potash	14.5	1.9	8.2	0.5	0.5	2.7	0.4	<LLD	0.2	1.4	<LLD	2.6	0.2	2.1	1.0	1.0
JXL39	Blue	Waste	4	m-Na-Al	89.1	7.0	26.2	3.0	0.8	2.4	0.5	2.4	0.2	1.2	0.3	<LLD	0.2	12.9	39.9	26.1
JXL41	Aqua	Waste	4	m-Na-Al	50.8	5.6	20.7	2.5	1.0	2.7	0.3	1.6	0.1	0.7	0.3	2.0	0.5	15.0	13.5	4.7
JXL43	Dark blue	Waste	4	v-Na-Ca	11.5	1.3	5.7	1.3	0.4	1.2	0.3	2.1	0.4	0.8	0.3	<LLD	<LLD	2.9	1.5	0.6
JXL44	Blue	Waste																		
JXL46	Blue	Waste	4	v-Na-Ca	42.5	4.4	18.5	4.0	0.3	4.4	0.5	2.3	0.3	0.7	0.3	<LLD	0.3	3.0	5.3	0.6
JXL47	Red	Waste	4	v-Na-Ca	13.2	1.5	6.9	0.4	0.4	0.9	0.1	1.2	0.2	0.2	<LLD	1.4	0.2	1.8	1.5	0.6
JXL48	Yellow	Waste	4	m-Na-Al	20.4	2.0	8.0	1.3	0.8	2.2	0.3	1.4	0.4	0.9	0.4	2.5	0.3	6.2	2.4	13.2
JXL49	Aqua	Waste	4	m-Na-Al	91.9	8.8	29.5	2.7	1.1	1.7	0.3	1.9	0.2	1.4	<LLD	1.4	0.2	11.3	37.8	18.8

compositions – JXL41 has 0.2 wt% CuO and 1.2 wt% FeO, while JXL49 has negligible amounts of CuO and FeO. The two samples are fully transparent, with no silica relics but a few zircons. The lack of bubbles and silica relics shows that the microstructure of the aqua glass waste does not resemble the microstructure of the glass beads (in other colours) from Jiuxianglan. Although one can argue that the aqua glass could be used as a base glass for the addition of colouring compounds in order to produce different coloured beads, there are no supporting archaeological finds related to colouring at the site, nor aqua coloured beads, and the microstructure suggests a fully melted glass, with few relics, which is unlike most of the beads analysed.

Red glass beads and waste

The six red glass beads analysed are all m-Na-Al glass, while the single red glass waste rod has a v-Na-Ca composition (Fig. 3). The significant difference between the base glass compositions of the red beads and waste indicates that the glass beads were not made using the glass represented by the red waste at Jiuxianglan, despite both the beads and waste showing a similar microstructure, with copper sulphide particles of around 10 μm distributed within the glass matrix (Wang et al. submitted).

The minor and trace elemental patterns in the red beads and waste also shows some differences. Zr is higher in the glass beads, at around 300–600 ppm, which is typical of m-Na-Al glass, while in the red v-Na-Ca glass waste rod a Zr content as low as 60 ppm is detected. In the red v-Na-Ca glass *waste*, higher concentration of Sb (110 ppm) and Mn (0.5 wt%) are found, compared to the red *beads* made of m-Na-Al glass (Sb < 20 ppm and Mn < 0.1 wt%). This difference is frequently observed between the v-Na-Ca and m-Na-Al glass in Iron Age samples from Taiwan, and whether this is related to the differences in raw materials or production process between m-Na-Al and v-Na-Ca glass is not yet known (Wang 2016: 191). However, the different glass compositions of red beads of an m-Na-Al composition and the red waste which has a v-Na-Ca composition analysed here has demonstrated that these red glass beads do not derive from the waste found.

Orange glass beads

No orange glass waste was found at Jiuxianglan. Three orange glass beads were analysed and all have an m-Na-Al glass composition. It is noted that, although the orange and red glass bead are all probably coloured by cuprite, the CuO wt% in the orange glass (5–8 wt%) is much higher than that in the red glass (< 2 wt%), which may suggest that a larger amount of copper-containing raw materials was used for producing orange glass. Elevated concentrations of PbO and SnO_2 are also found in the orange glass (PbO 1–1.5 wt% and SnO_2 0.4–

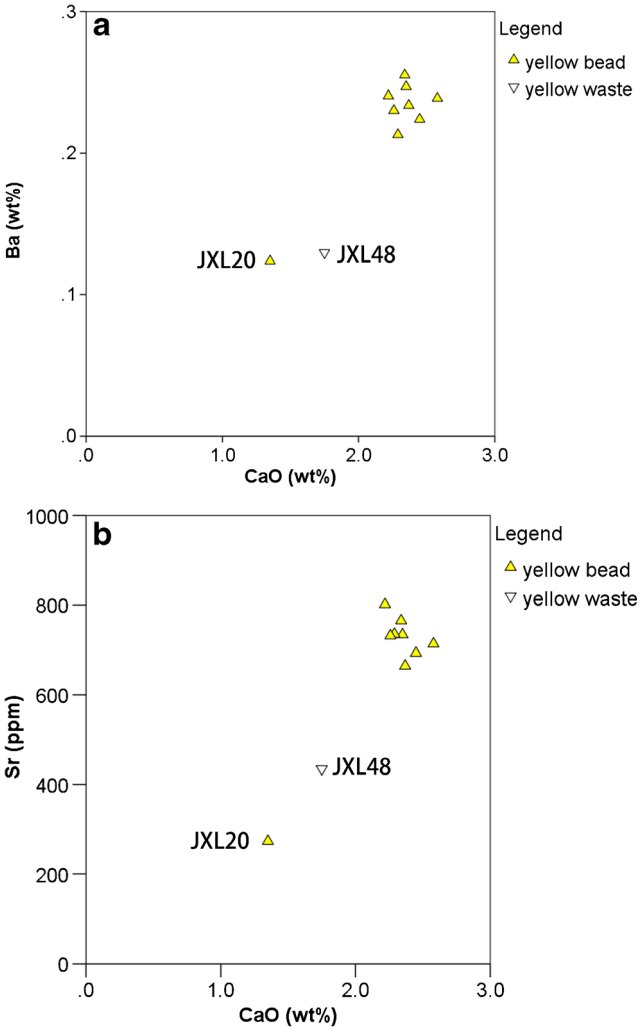

Fig. 4 **a** CaO-Ba and **b** CaO-Sr bi-plots of yellow m-Na-Al glass from Jiuxianglan

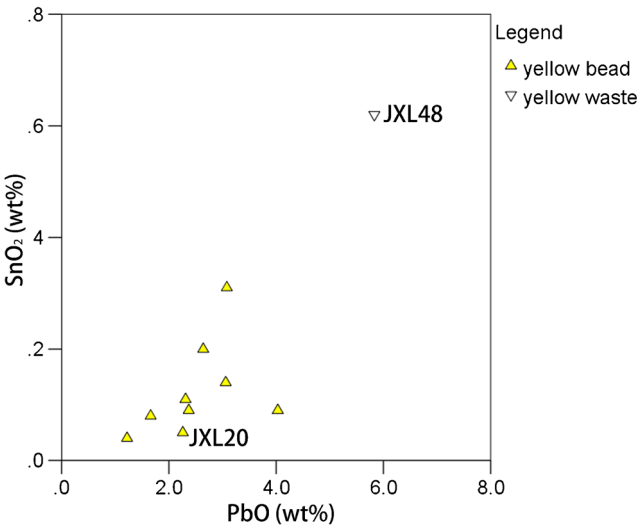

Fig. 5 PbO-SnO_2 bi-plot of yellow m-Na-Al glass from Jiuxianglan

1.3 wt%) compared to the red glass (PbO < 1 wt% and SnO_2 < 0.1 wt%), which may suggest different sources of copper-containing raw materials used in colouring the red and orange glass beads excavated at Jiuxianglan (Wang et al. submitted).

Green glass beads

Nine green glass beads were analysed, and all are m-Na-Al glass, coloured by copper oxide and lead tin oxide, with CuO of 0.5–1.5 wt%, PbO of 2–6 wt% and SnO_2 < 0.5 wt%. The CuO is detected in the matrix by EDS analysis, while the crystals of lead tin oxide are distributed throughout the matrix, which corresponds to the yellow streaks observed under the optical microscope (Wang 2016: 173–175). This suggests the green colour may be a result of mixing blue (coloured by copper) and yellow colourants, and the opacity derived from the lead tin oxide. Unfortunately, although green glass waste was found on site, no sampling of this waste was permitted for this research, and therefore it is not possible to compare the chemical compositions and microstructure of the green glass beads and waste.

Discussion: beads and waste in their archaeological context

Beadmaking at Jiuxianglan?

The results presented show that the manufacturing processes are different for the beads and that evidenced in the glass waste. The presence of drawn beads, but glass waste showing relics of manufacture using the wound method, indicates that the beadmaking methods identified in glass bead and glass waste do not match. The evidence from the chemical and microstructural analysis also does not support the assumption that these glass beads were locally made using the glass represented by the waste here. This is because (1) the raw materials are not fully consistent between the beads and waste fragments; there is an m-Na-Al glass bead but no m-Na-Al waste and perhaps more importantly v-Na-Ca glass waste has been found but no beads in this composition, (2) the colouring recipes generally do not match (e.g. such as the case of yellow glass), and (3) the manufacturing processes do not appear to be the same (e.g. such as the case of blue glass). Therefore, taking this evidence together there is a paradox between glass beads and waste here. Several factors which may explain this are discussed below.

Sampling bias is one possible reason. Only a total of 36 bead samples were selected in this research, while thousands of glass beads were unearthed from Jiuxianglan. In terms of glass waste, 8 samples were analysed and around 140 pieces of glass waste were found. However, visual observation of other un-analysed bead samples suggests that most of the glass beads from Jiuxianglan appear to be drawn beads. This shows

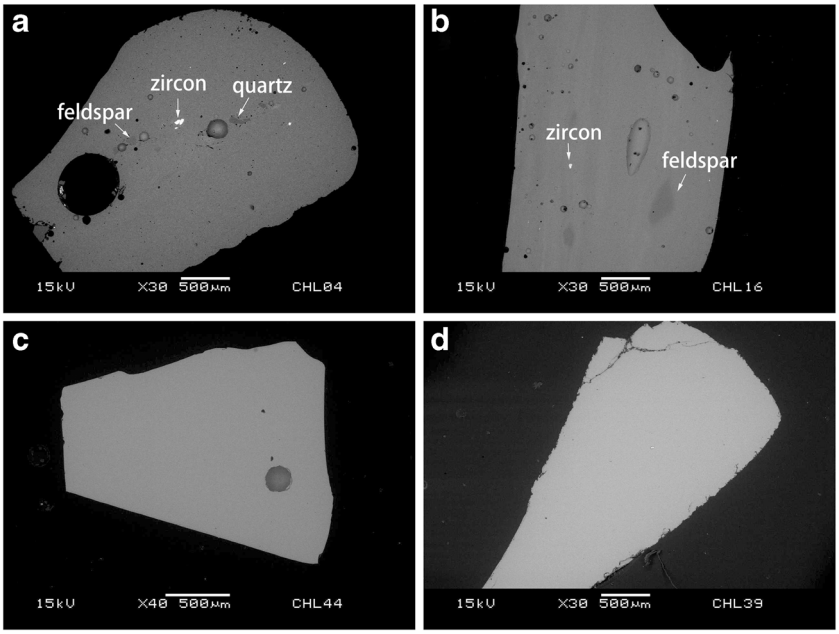

Fig. 6 Selected microstructure of light blue m-Na-Al glass, showing the difference between beads (**a**, **b**) and waste (**c**, **d**); in the beads, it is observed the various sizes of bubbles and remains of minerals as well as the heterogeneous chemical composition of the matrix, while the waste exhibits a much more homogeneous matrix

an inconsistency with the waste identified here which was produced using the wound method and the bead on a mandrel reported by Lee (2005a) which is typical of wound bead production. Thus, compositionally and structurally none of the analysed beads and waste match, and even with the relatively small sample permitted for analysis some correspondence between the beads and waste might be expected.

Other possible reasons that lead to the anomaly between glass beads and waste must take into consideration the spatial and temporal distribution of the beads and waste at the site, which may suggest that the presence of *drawn* glass beads and *wound* beadmaking at Jiuxianglan may not be contemporary.

Glass beads were found predominantly in the coastal area at Jiuxianglan, where it was suggested pyrotechnological activities, including glass beadmaking, were practiced. The pyrotechnological activity was evidenced by an area containing a gravel structure and burned soil (Fig. 1). A more detailed investigation into the spatial distribution of the glass beads and waste within this area has shown a more southward distribution of the glass waste (Wang 2016: 220–224). A more concentrated distribution and greater number of finished beads were found near the gravel structure and these overlap the burned soil shown in Fig. 1 (near T3P36, see discussion below). This area also contains a dense and thick deposit of artefacts and waste which may be related to *other* pyrotechnological activities (Lee 2015a: 140–141). In contrast, most of the glass waste was found south of the area of burned soil (trenches T3P38-T3P40). Thus, although bead production can leave little physical evidence of burning in the deposits and so might not be evidenced at either the bead or waste locations, the spatial distribution of the beads and waste suggests the two are not necessarily associated.

C-14 dating of the areas near T3P36 (which shows the deposition of burned soil and dense distribution of finished *drawn* glass beads) indicates a period earlier than sixth century AD, while the data from T3P39 (where most *wound* glass waste were found) suggests a later period of around seventh century AD (Lee 2015a: 146). Thus, the inconsistency in manufacturing methods and composition between glass beads and waste in this research may be a feature of chronological differences. The evidence presented here suggests that *wound* beadmaking at Jiuxianglan may be a later development, and post-dates the deposition of the *drawn* beads, which may be imported. Without the analysis of more beads from the sites, the possibility of local production cannot be fully ruled out, although our visual examination of the other beads excavated from the site suggests these too were likely to be produced by the drawn method and so do not match the waste found.

The overlap of finished beads and burned soil (which may be related to production activity) in nearby trenches, however, is more questionable and should take into consideration of the topography of this area. Figure 1b shows the inclination of the deposition and burned soil (grey area in the archaeological deposition) from northeast to southwest (in Fig. 1b right to left). This may reflect a complex depositional sequence of glass beads and burned soils as a result of human behaviour *and* natural formation processes. One possible reason for the inclined deposition may be the active disposal of the burned soil and the waste relating to pyrotechnology from the higher levels close to T3P36 (human behaviour) (see the grid of trench in Fig. 1a). Another factor may be the natural movement of the sand dune which may have resulted in the dumping or movement of the deposit from northeast to southwest (natural formation process) (Lee 2015a: 140–141). Therefore, the overlap of glass

beads and burned soils close to T3P36 may not be a contemporaneous event but a sequential one, and considering the formation process of the site, it is tentatively suggested by the excavator that the areas near T3P36 (where the elevation is higher) may reflect the earlier deposit, while the southward lower parts may be later. This sequence of events corresponds to the C-14 results discussed above (Lee 2015a: 140–141).

Thus, this additional evidence indicates that there are still more questions than answers relating to the beadmaking activities at Jiuxianglan. This may be partly resolved by more detailed investigation on a greater number of beads, their contexts and relationship to other finds, especially those which are related to the pyrotechnological process. Together, this will help define the role of Jiuxianglan, and any potential changes in its role in this period spanning over a thousand years. That the beads and waste do not correspond in terms of composition, style or context does not mean that beadmaking did not occur on the site at some time, just that these two sets of evidence do not seem to be contemporaneous.

The origin, development and introduction of bead making methods

Another question arising from this research is the possible origin of wound beadmaking methods, such as those (tentatively) seen at Jiuxianglan. It has been suggested that most Indo-Pacific glass beads were made by the drawn method (Francis 1990), which contrasts with those produced by the wound method seen in the glass waste at Jiuxianglan. Although evidence of other non-drawn beadmaking methods have been seen elsewhere, such as Khao Sam Kaeo (mid-late 1st millennium BC) (Lankton et al. 2008b; Bellina 2014) and Khao Sek (Dussubieux and Bellina in press) in Thailand and East Java (the mid-1st millennium AD), the beadmaking technology at Khao Sam Kaeo and Khao Sek is by the cold-working lapidary method rather than the wound method, and in East Java it is the mosaic method that was used to produce the Jatim glass bead. At present, there are no other sites where wound beadmaking methods have been securely identified around the South China Sea in this period, and hence there is no evidence the technique was transferred from Southeast Asia to Jiuxianglan in southeastern Taiwan.

One possible origin for this wound bead technology is China where the source of the wound method has been proposed (Francis 2002: 76–78). However, Chinese wound beads from around the South China Sea region (Francis 2002: 76–78) are generally found much later (ca. twelfth century onwards) than the date of Jiuxianglan (ca. third century BC-eighth century AD). The archaeological artefactual evidence also does not point to direct interaction between China and Jiuxianglan in the 1st millennium AD. Therefore, the potential source of the knowledge of wound beadmaking technology at Jiuxianglan remains unclear, unless it was an indigenous development.

Conclusion

Jiuxianglan was assumed to be a possible centre of glass beadmaking and bead exchange in Iron Age Taiwan. It is demonstrated in this research, however, that the glass beads and waste do not match in terms of the beadmaking methods, raw materials, manufacturing processes and their spatial and temporal distribution. The current results seem to suggest the possibility that the glass beads analysed here were imported. This anomaly however does not necessarily rule out the possibility of bead production at Jiuxianglan at a later date than the deposition of the beads, but currently there is no strong indication that the finished beads were locally produced at Jiuxianglan.

Waste glass, indicative of wound bead production, has been found dating to around the sixth century, but it is unclear whether the wound method of bead production at Jiuxianglan was a local development or the result of transferred knowledge. Through comparison to other known areas of bead production in the South China Sea region it can be seen that there were diverse methods of beadmaking practiced in local areas around the South China Sea and the evidence from Jiuxianglan may be part of this complex picture. The picture emerging from this analysis is that Jiuxianglan probably took part in the import of exotic glass beads in the earlier period and later developed bead production at the site. This may indicate a potential change in cultural, social or economic activities at Jiuxianglan within a thousand years.

Acknowledgements We would like to thank Dr. Laure Dussubieux of the Field Museum of Natural History, Chicago for the consultation and discussion during carrying out this research. Special thanks are also given to Mr. Yu-Shiang Wang and Ms. Hui-Ho Hsieh in the Institute of Earth Sciences, Academia Sinica for helping sample preparation and instrumental operation at the Institute of Earth Sciences, Academia Sinica. We also thank Dr. Hsiao-Chun Hung in the Australian National University for the advice related to the South China Sea interaction network. Thanks are also given to the two anonymous reviewers, whose comments help improve the content of this paper.

References

Bellina B (2014) Maritime silk roads' ornament industries: socio-political practices and cultural transfers in the South China Sea. Camb Archaeol J 24(03):345–377. https://doi.org/10.1017/S0959774314000547

Brill RH (1999) Chemical analyses of early glasses, vol 2. The Corning Museum of Glass, New York

Dussubieux L, Bellina B (in press) Glass ornament production and trade polities in the Upper-Thai Peninsula during the early iron age archaeological research in Asia. https://doi.org/10.1016/j.ara.2017.08.001

Dussubieux L, Gratuze B (2010) Glass in Southeast Asia. In: Bellina B, Bacus EA, Pryce TO, Christie JW (eds) 50 years of archaeology in Southeast Asia: essays in honour of Ian Glover. River Books, Bangkok, pp 246–259

Dussubieux L, Robertshaw P, Glascock MD (2009) LA-ICP-MS analysis of African glass beads: laboratory inter-comparison with an emphasis on the impact of corrosion on data interpretation. Int J Mass Spectrom 284(1-3):152–161. https://doi.org/10.1016/j.ijms.2008.11.003

Francis P (1990) Glass beads in Asia: part I. Introduction Asian. Perspectives 28:1–21

Francis P (2002) Asia's maritime bead trade: 300 B.C. to the present. University of Hawai'i Press, Honolulu

Freestone IC, Leslie KA, Thirlwall M, Gorin-Rosen Y (2003) Strontium isotopes in the investigation of early glass production: byzantine and early Islamic glass from the near east. Archaeometry 45(1):19–32. https://doi.org/10.1111/1475-4754.00094

Gratuze B (1999) Obsidian characterization by laser ablation ICP-MS and its application to prehistoric trade in the Mediterranean and the near east: sources and distribution of obsidian within the Aegean and Anatolia. J Archaeol Sci 26(8):869–881. https://doi.org/10.1006/jasc.1999.0459

Hung H-C, Bellwood P (2010) Movement of raw materials and manufactured goods across the South China Sea after 500 BCE: from Taiwan to Thailand, and back. In: Bellina B, Bacus EA, Pryce TO, Christie JW (eds) 50 years of archaeology in Southeast Asia: essays in honour of Ian Glover. River Books, Bangkok, pp 234–245

Hung HC, Chao CY (2016) Taiwan's early metal age and Southeast Asian trading systems. Antiquity 90(354):1537–1551

Lankton J, Diamanti J, Kenoyer JM (2003) A bead timeline. Volume I: Prehistoty to 1200 CE. The Bead Society of Great Washington, Washington DC

Lankton J, Dussubieux L, Rehren T (2008) A study of mid-first millennium CE Southeast Asian specialized glass beadmaking traditions. In: Bacus E, Glover I, Sharrock P (eds) Interpreting Southeast Asia's past: monument, image and text: selected papers from the 10th International Conference of the European Association of Southeast Asian Archaeologists. University Press, Singapore, pp 335–356

Lee K-S (2005a) Glass materials from Jiuxianglan and the relevant research questions. Paper presented at the Foreign Substances in Taiwan: Beads and Penannular Jade Ring. Institute of History and Philology, Academia Sinica, Taipei 2005.10.22-23 (unpublished, in Chinese)

Lee K-S (2005b) The report of rescue excavation at Jiuxianglan in Taitung County. Taitung County Government, Taitung (unpublished, in Chinese)

Lee K-S (2007) The report of 2nd rescue excavation at Jiuxianglan in Taitung County. Taitung County Government, Taitung (unpublished, in Chinese)

Lee K-S (2010) The report of rescue excavation at Jiuxianglan in Taitung: cultural layers and funerary vol 1. Taitung County Government and National Museum of Prehistory, Taitung (unpublished, in Chinese)

Lee K-S (2015a) The report of rescue excavation at Jiuxianglan in Taitung: pottery from cultural layers vol 3. Taitung County Government and National Museum of Prehistory, Taitung (unpublished, in Chinese)

Lee K-S (2015b) The sandstone casting mould from Jiuxianglan: a pilot study of the meaning and origin. Paper presented at the Annual Conference of Taiwan Archaeologists 2016, Taipei, Institute of History and Philology, Academia Sinica, 2015.05.01–02 (unpublished, in Chinese)

Liu Y-C (2011) The history of Taiwan: archaeological records of the inhabitants vol 3. Taiwan Historica, Nantou (in Chinese)

Liu Y-C, Tseng C-M, Kao Y-J (1994) Report of the survey on cultural sites: the site selection of the Southern Cross-Island Highway. Ministry of Transportation and Communications Taiwan Area National Expressway Engineering Bureau, Taipei (unpublished, in Chinese)

Mielke JE (1979) Composition of the Earth's crust and distribution of the elements. In: Siegel FR (ed) Review of research on modern problems in geochemistry. UNESCO Report, Paris, pp 13–37

Pearce NJG, Perkins WT, Westgate JA, Gorton MP, Jackson SE, Neal CR, Chenery SP (1997) A compilation of new and published major and trace element data for NIST SRM 610 and NIST SRM 612 glass reference materials. Geostand Newslett 21(1):115–144. https://doi.org/10.1111/j.1751-908X.1997.tb00538.x

van der Sleen WGN (1967) A handbook on beads. George Shumway Publisher, York, PA

Wagner B, Nowak A, Bulska E, Hametner K, Günther D (2012) Critical assessment of the elemental composition of Corning archeological reference glasses by LA-ICP-MS. Anal Bioanal Chem 402(4):1667–1677

Wang K-W (2016) Cultural and socio-economic interaction reflected by glass beads in early Iron Age Taiwan. PhD Thesis, University of Sheffield

Wang K-W, Jackson C (2014) A review of glass compositions around the South China Sea region (the late 1st millennium BC to the 1st millennium AD): placing Iron Age glass beads from Taiwan in context. J Indo-Pacific Archaeol 34:51–60. https://doi.org/10.7152/jipa.v34i0.14701

Yang H, Lee K-H, Chen W (2012) The application of petrographic analysis to archaeological research: examples from the artifacts and sherds of Chiu Hsiang Lan site, Taitung, Taiwan. J Austronesian Stud 南島研究學報 3:71–88 (in Chinese)